Concentration fluctuations and boson peak in a binary metallic glass: A generalized collective modes study

Taras Bryk and Ihor Mryglod

Institute for Condensed Matter Physics, National Academy of Sciences of Ukraine, 1 Svientsitskii Street, UA-79011 Lviv, Ukraine and Institute of Applied Mathematics and Fundamental Sciences, National Technical University of Lviv, UA-79013 Lviv, Ukraine

(Received 11 August 2010; revised manuscript received 8 October 2010; published 22 November 2010)

It is shown that longitudinal and transverse concentration dynamic structure factors of a metallic binary glass $Mg_{70}Zn_{30}$ obtained by molecular dynamics (MD) simulations contain pronounced low-frequency peaks, that correspond to boson-peak modes. With a purpose of theoretical analysis of MD-derived time-correlation functions an extended approach of generalized collective modes (EGCM) is proposed, that permits treatment of slow collective processes in glasses. The EGCM eigenvalues are analyzed for estimation of dispersion of collective excitations in the binary glass. Low-frequency collective eigenmodes with very flat dispersion corresponding to the region of boson peak are obtained among the EGCM eigenvalues. An eigenvector analysis, performed for estimation of contributions from the collective modes to dynamic structure factors, supports strong contribution of boson-peak modes to concentration dynamic structure factors of $Mg_{70}Zn_{30}$ glass.

DOI: 10.1103/PhysRevB.82.174205 PACS number(s): 61.20.Ja, 61.20.Lc, 62.60.+v

I. INTRODUCTION

Vibrational dynamics in glasses is one of the most attractive problems of modern statistical physics. Despite of success of mode coupling theory (MCT) (Ref. 1) in description of glass transition and nonpropagating relaxation processes in supercooled liquids and glasses[2,3] much less attention was paid to theoretical studies on dispersion of collective excitations in glass systems. There are many qualitative theoretical explanations of specific features of dispersion and damping of acoustic excitations in glasses and emergence of a low-frequency excess on the density of vibrational states (boson peak),[4–8] while numerical studies of collective excitations in glasses are mainly performed by oversimplified fit procedures or by instantaneous mode analysis within harmonic approximation. Moreover there exist several points of view on the origin of the boson peak. One connects it to the renormalization of the dispersion law of acoustic excitations in the region of the Ioffe-Regel limit.[9] Grigera *et al.*[10] claimed that the boson peak is the signature of a phase transition from a phase with dominated energy landscape minima (with phonons) to a phase dominated by energy saddle points (without phonons). Another theory states that some specific only for the glass state soft modes cause the boson peak.[11] Other theoretical approaches associate the boson peak with renormalized optic transverse modes[12] or more complex processes involving so-called ripplon modes.[13]

Molecular-dynamics (MD) simulations can shed light on the origin of boson peak in glasses via analysis of derived in MD dynamic structure factors $S(k,\omega)$, where k and ω are the wave number and frequency, respectively. According to hydrodynamic theory of amorphous solids[14] the side peaks of $S(k,\omega)$ are associated solely with propagating acoustic collective modes. In binary glasses another type of collective excitations, the opticlike modes, yield a high-frequency peak on the shape of concentration current spectral function.[15] Following the frequency of peak positions of $S(k,\omega)$ for different wave numbers one can estimate the dispersions of collective propagating processes directly from MD simulations. Hence, in case of observation of some peaks of $S(k,\omega)$ in the frequency range of the excess of vibrational density of states corresponding to boson peak one can potentially estimate the wave-number region of existence of the low-frequency collective processes, features of their dispersion and damping.

However, there is some lack of studies focused on theoretical analysis of computer experiments and density-density time-correlation functions, in particular, obtained in MD simulations, having the purpose of estimation of dispersion and damping of collective excitations in glass systems. Mainly purely numerical studies of MD-derived dynamic structure factors[16–19] and the normal-mode analysis[20–22] are actively used for exploration of collective dynamics of disordered solids. Theoretical studies focused on analysis of short-time behavior of density-density time-correlation functions or other theoretical schemes of analysis of collective excitations for realistic glass systems from MD simulations are almost absent in the literature. For glasses there do not exist reliable fit procedures for analysis of MD-derived time-correlation functions based on a memory-function approach as it is widely used in case of collective dynamics in liquids.[23] Mainly one can find in the literature a simplified analysis based on damped harmonic oscillator model or a standard procedure of direct estimation of dispersion of collective excitations via side peak positions of dynamic structure factors $S(k,\omega)$ or maxima positions of longitudinal current spectral functions $C^L(k,\omega)$. However, very frequently the low-frequency peaks of dynamic structure factors, that can shed light on the long-wavelength behavior of boson-peak modes, are not seen in the shape of $S(k,\omega)$ because either of their weak intensity or inability to separate boson-peak contribution on the background of well-pronounced acoustic peak in the region of small wave numbers. Therefore it is not known to date how would behave the frequency of boson-peak modes in long-wavelength limit if they do exist on nanoscales.

Recently several reports appeared, in which the transverse dynamics in monoatomic glass systems were analyzed from the "transverse" dynamic structure factors $S^T(k,\omega)$.[24,25] The

authors formally used the exact relation between longitudinal current density and particle density (continuity equation) to obtain from the transverse current spectral function a transverse analogue of the dynamic structure factor

$$S^{L,T}(k,\omega) = \frac{k^2}{\omega^2} C^{L,T}(k,\omega). \quad (1)$$

The analysis of transverse analogue of dynamic structure factor $S^T(k,\omega)$ can yield additional information about features of collective excitations in disordered systems.

For the study of collective dynamics in liquids several methods of analysis of MD-derived time-correlation functions were developed.[23,26,27] One of the most successful of them is an approach of generalized collective modes (GCM) (Refs. 28 and 29) that permits to represent dynamic structure factors in wide ranges of wave numbers and frequencies as a separable sum of contributions from hydrodynamic (sound excitations, thermal and viscous relaxations) and *nonhydrodynamic* (that do not survive on macroscopic length and time scales) processes. The GCM approach was formulated[29] as a generalization of hydrodynamics with systematic improvement of short-time behavior of time-correlation functions by treating on the same footing additional short-time dynamic variables along with hydrodynamic ones. Since the short-time dynamic variables are chosen in the GCM approach as successive time derivatives of hydrodynamic variables the GCM representation of time-correlation functions coincide with MD-derived time-correlation functions within several first terms of the short-time expansion, that is equivalent to precision of several first frequency moments of corresponding dynamic structure factors. It was shown that for regular (nonsupercooled) liquids in order to reproduce the MD-derived density-density time-correlation function with very good quality it is enough to restrict the GCM extended set of dynamic variables by the first-time derivatives of currents and energy density, that corresponds to precision within the fourth frequency moment of $S(k,\omega)$,[30,31] although studies with much higher number of dynamic variables were performed too.[32,33] Numerous analytical results obtained within the GCM approach for nonhydrodynamic collective modes permitted to construct the theory of opticlike excitations,[34,35] heat waves,[33] and wave-number-dependent structural relaxation in liquids,[30] completely supported by MD simulations. Namely, the presence of the first-time derivatives of mass and concentration currents, which are connected with elastic properties of the liquids, among the dynamic variables for construction of the generalized hydrodynamic matrix[29] and estimation of corresponding dynamic eigenmodes in the system, permits a straightforward and correct way for description of acoustic and optic excitations in liquids within the GCM approach. This makes an essential difference with the level of treatment of short-time processes in MCT because the high-order sum rules like equivalence of the fourth frequency moment of dynamic structure factors are not directly incorporated into MCT.[2] Very recently the GCM approach allowed us to solve a problem of "fast sound"[36] in binary liquids with disparate masses such as Li_4Pb (Ref. 37) and Li_4Tl (Ref. 38) and to find a crossover in mode contributions from the high- and low-frequency branches of collective excitations by approaching the hydrodynamic regime. The problem of fast sound was known from MD simulations of Li_4Pb (Ref. 36) and inelastic neutron-scattering experiments on Li_4Pb and Li_4Tl,[39] and despite of initial analysis by MCT (Ref. 36) it was not clear until recently how the high-frequency branch would behave in the long-wavelength limit.

Two features of the regular GCM approach do not permit its direct application in theoretical studies of collective dynamics in glasses: (i) the extended set of dynamic variables in the GCM approach is generated from the hydrodynamic set by systematic extending it with solely short-time orthogonal variables having a purpose to represent correctly the high-frequency collective dynamics in liquids; (ii) the highest memory functions are taken in Markovian approximation, that is well justified for liquid state when the density-density time-correlation functions decay exponentially on large times. Hence the regular GCM approach is not directly suitable for description of the low-frequency dynamics in glasses and supercooled liquids with slow decay of memory effects.

In this paper we will show how the GCM approach can be extended for applications to glasses. We will make use of a brilliant idea by Omelyan and Tokarchuk[40] on application of time moments of relevant time-correlation functions to description of main slow collective processes, that was used firstly in the study of dielectric relaxation in liquid water.[40,41] The remaining paper is organized as follows. In the next two sections we report our extended GCM (EGCM) approach for glasses and give details of MD simulations. Analysis of time-correlation functions of a binary metallic glass $Mg_{70}Zn_{30}$ is performed by the EGCM approach and compared with regular viscoelastic (VE) approximation. Wave-number-dependent mode strengths of different collective modes are analyzed in order to find out dominant collective modes contributing to total and concentration dynamic structure factors. Conclusions of this study are given in the last section.

II. DETAILS OF MOLECULAR-DYNAMICS SIMULATIONS

We simulated molten and glass $Mg_{70}Zn_{30}$ system by classical molecular dynamics having two systems of 1000 and 8000 particles in cubic boxes under periodic boundary conditions in microcanonical ensemble. The time step in simulations was 5 fs. We made use of two-body effective potentials for $Mg_{70}Zn_{30}$, proposed in Ref. 15 and tested them in previous studies of calculations of static and dynamic properties of liquid $Mg_{70}Zn_{30}$. The glass system was prepared from the liquid configuration by a quench with the rate $\sim 10^{13}$ K/s down to the room temperature. The subsequent equilibration over 20 ps was performed in order to anneal away any transient structures. The final glass state was controlled by the stable long-time plateau of partial density-density time-correlation functions.

Molecular-dynamics simulations were performed over 240 000 time steps of production run in order to obtain the time evolution of all relevant dynamical variables, which formed the basis set in our many-variable GCM approach.

For each k point sampled in MD simulations all the static and time correlation functions were averaged over all possible directions of corresponding wave vectors. Numerical Fourier transform of obtained time-correlation functions with subtracted nonergodicity factors were performed by means of standard codes. The shape of MD-derived time-correlation functions and the spectra of eigenvalues were analyzed with different models within the extended GCM method for longitudinal and transverse dynamics.

III. EXTENDED APPROACH OF GENERALIZED COLLECTIVE MODES FOR GLASS DYNAMICS

The standard GCM approach permits to solve the generalized Langevin equation, represented in matrix form and generated on a chosen set of N_v dynamic variables, as an eigenvalue problem. Complex-conjugated pairs of eigenvalues correspond to propagating in the system collective modes with wave number k and phase speed estimated from the dispersion $\omega_\alpha(k)=Im[z_\alpha(k)]$ while purely real eigenvalues describe nonpropagating relaxation processes. Corresponding eigenvectors, associated with some $z_\alpha(k)$ eigenvalue, define its contributions to all time-correlation functions or dynamic structure factors of interest (see Ref. 29).

Usually the basis set of N_v dynamic variables for construction of matrix representation of the generalized Langevin equation is generated by extending the set of hydrodynamic variables, that describe fluctuations of conserved quantities, by their first-time derivatives, which are aimed to describe correctly short-time fluctuations. Since the static correlation between a dynamic variable $A_i(k,t)$ and its first-time derivative due to symmetry reasons for equilibrium classical systems is zero[26]

$$\langle A_i^*(k,0)\dot{A}_i(k,0)\rangle \equiv 0, \tag{2}$$

it is possible to extend the hydrodynamic set by more short-time *orthogonal* dynamic variables and hence try to improve hydrodynamic description of collective processes by accounting for short-time dynamics. Here and henceforth the overdots mean corresponding order of time derivatives.

For binary liquids the hydrodynamic set of variables for description of longitudinal dynamics consists of four dynamic variables[42]

$$\mathbf{A}^{(4hyd)}(k,t)=\{n_t(k,t),n_x(k,t),J_t^L(k,t),e(k,t)\}, \tag{3}$$

where the kth spatial-Fourier components of total density $n_t(k,t)$ and mass-concentration density $n_x(k,t)$ of the system, composed of $N=N_A+N_B$ particles with instantaneous positions $\mathbf{r}_i^\alpha(t)$ and velocities $\mathbf{v}_i^\alpha(t)$, are constructed from the partial particle densities

$$n_\alpha(k,t)=\frac{1}{\sqrt{N}}\sum_{j=1}^{N_\alpha} e^{i\mathbf{k}\mathbf{r}_j^\alpha(t)} \quad \alpha=A,B \tag{4}$$

in the following way:

$$n_t(k,t)=n_A(k,t)+n_B(k,t),$$

$$n_x(k,t)=\frac{m_A m_B}{\bar{m}^2}[c_B n_A(k,t)-c_A n_B(k,t)]. \tag{5}$$

Here m_α, $c_\alpha=N_\alpha/N$, and $\bar{m}=c_A m_A+c_B m_B$ are atomic mass of species, concentration, and average mass, respectively. The other hydrodynamic variables in Eq. (3) are the Fourier components of longitudinal component of total mass-current density

$$J_t^L(k,t)=\frac{1}{\sqrt{N}}\frac{1}{k}\left[\sum_{j=1}^{N_A} m_A\mathbf{k}\mathbf{v}_j^A e^{i\mathbf{k}\mathbf{r}_j^A(t)}+\sum_{j=1}^{N_B} m_B\mathbf{k}\mathbf{v}_j^B e^{i\mathbf{k}\mathbf{r}_j^B(t)}\right]$$
$$\equiv J_A^L(k,t)+J_B^L(k,t) \tag{6}$$

and energy density

$$e(k,t)=\frac{1}{\sqrt{N}}\sum_{j=1}^{N}\varepsilon_j e^{i\mathbf{k}\mathbf{r}_j(t)}, \tag{7}$$

where ε_j is the single-particle energy of jth particle. The hydrodynamic variables [Eqs. (5)–(7)] correspond to fluctuations of conserved quantities and can be easily sampled in MD simulations. We would like to remind that the concentration current $\mathbf{J}_x(k,t)$ in contrast to total mass-current does not belong to hydrodynamic variables. In order to account for nonhydrodynamic processes in dynamics of binary liquids within the GCM approach one has to apply for solving the generalized Langevin equation an extended set of dynamical variables

$$\mathbf{A}^{(N_v)}(k,t)=\{n_t(k,t),n_x(k,t),J_t^L(k,t),e(k,t),$$

$$J_x^L(k,t),\dot{J}_t^L(k,t),\dot{J}_x^L(k,t),\dot{e}(k,t),\ddot{J}_t^L(k,t),\ddot{J}_x^L(k,t),\ddot{e}(k,t),\ldots\}. \tag{8}$$

The chosen set of N_v dynamical variables is used for construction of a generalized hydrodynamic matrix $\mathbf{T}(k)$, eigenvalues of which define the spectrum of collective propagating and relaxing eigenmodes in the system. The generalized hydrodynamic matrix $\mathbf{T}(k)$ in GCM approach[29] is expressed as

$$\mathbf{T}(k)=\mathbf{F}(k,0)\tilde{\mathbf{F}}^{-1}(k,0).$$

Here $\mathbf{F}(k,t=0)$ is a $N_v\times N_v$ matrix of static correlation functions with elements

$$F_{ij}(k,t=0)=\langle A_i^*(k,t=0)A_j(k,t=0)\rangle, \tag{9}$$

where the asterisk means complex conjugation and $\tilde{\mathbf{F}}(k,0)$ is corresponding matrix of Laplace-transformed time-correlation functions $\tilde{\mathbf{F}}(k,z)$ at $z=0$.

For the case of glass dynamics it is important to note that the theoretical scheme must account for the processes, which are even slower than the hydrodynamic ones. Another feature of collective dynamics in glass can be taken into account: usually there is no need to consider heat fluctuations because they are almost decoupled from density fluctuations for glass systems. With all this in mind one may start our consideration of the collective dynamics of binary glass from the following VE basis sets of dynamic variables:

$$\mathbf{A}^{(6)}(k,t) = \{n_A(k,t), n_B(k,t), J_A^L(k,t), J_B^L(k,t), \dot{J}_A^L(k,t), \dot{J}_B^L(k,t)\} \tag{10}$$

for longitudinal dynamics and

$$\mathbf{A}^{(4T)}(k,t) = \{J_A^T(k,t), J_B^T(k,t), \dot{J}_A^T(k,t), \dot{J}_B^T(k,t)\} \tag{11}$$

for transverse dynamics of the binary glass system. In order to take into account other slow processes we can represent them by making use of an integral relation as the following hierarchy:

$$I^1[n]_i(k,t) \equiv I[n]_i(k,t) = \int_{C_1}^{t} n_i(k,t')dt',$$

$$I^2[n]_i(k,t) = \int_{C_2}^{t} I[n]_i(k,t')dt',$$

$$\cdots$$

$$I^s[n]_i(k,t) = \int_{C_s}^{t} I^{s-1}[n]_i(k,t')dt', \tag{12}$$

where $i=A$, B, and C_s are arbitrary constants.[40] This corresponds to the general relations between slow and fast dynamical variables typical for the GCM approach

$$A_{fast}(k,t) = \frac{\partial}{\partial t} A_{slow}(k,t),$$

that permits to extend the hierarchy of orthogonal processes like in Eq. (2) for the case when the "fast" dynamic variable $A_{fast}(k,t)$ is the hydrodynamic one, for instance particle density or concentration density. It is obviously that these extended "slow" dynamic variables cannot be sampled directly in MD simulations. However, all the static averages and relevant correlation times[40] can be calculated from the MD-derived time-correlation functions, simply as

$$\langle I[n]_i^*(k) n_j(k)\rangle = \int_0^\infty F'_{n_i n_j}(k,t)dt \equiv \tau_{n_i n_j}(k),$$

$$\langle I^2[n]_i^*(k) n_j(k)\rangle = -\langle I[n]_i^*(k) I[n]_j(k)\rangle = \int_0^\infty t F'_{n_i n_j}(k,t)dt$$

$$\equiv \tau^{(2)}_{n_i n_j}(k), \tag{13}$$

where

$$F'_{n_i n_j}(k,t) = F_{n_i n_j}(k,t) - f_{n_i n_j}(k) \tag{14}$$

and $f_{n_i n_j}(k)$ are the nonergodicity factors, i.e., the values of long-time plateau for the corresponding time-correlation functions. Note that for the case of glass systems the integrals in Eq. (13) are well defined only for the case of time-correlation functions with subtracted nonergodicity factors in Eq. (14). By a suitable choice of constants C_s in Eq. (12) all the matrix elements of $\mathbf{T}(k)$ involving extended slow dynamic variables can be calculated by using the shifted by corresponding constants time-correlation functions in Eq. (14). It is obvious that the time derivatives of functions $F'_{n_i n_j}(k,t)$ and $F_{n_i n_j}(k,t)$ at origin, that define the short-time behavior, are identical.

The way of construction of slow dynamic variables in Eq. (12) permits to obtain the identical expression as in the regular GCM approach for the GCM representation of the time-correlation function in the form of sum of separable N_v mode contributions. For the case of the N_v-variable dynamic model for glass systems the GCM representation for density-density time-correlation functions can be written as followed:

$$F_{ij}^{(N_v)}(k,t) = \sum_{\alpha=1}^{N_v} G_{ij}^{\alpha}(k) e^{-z_\alpha(k)t} + f_{ij}(k). \tag{15}$$

In contrast to the mode-coupling theory, where the nonergodicity factors $f_{ij}(k)$ are obtained from a self-consistent solving of MCT equations, within the GCM approach they are taken directly from MD simulations. Each term in Eq. (15) corresponds to a contribution from a collective mode $z_\alpha(k)$. Among the N_v eigenmodes $z_\alpha(k)$ in Eq. (15) one can separate the hydrodynamic modes, fast nonhydrodynamic modes (such as structural relaxation and opticlike excitations) as well as ultraslow nonhydrodynamic modes. In the regular GCM approach with extended solely short-time dynamic variables up to the sth time derivative of hydrodynamic variables the GCM representations $F_{ij}^{(N_v)}(k,t)$ reproduce the MD-derived density-density time-correlation functions within the precision of first $2s+1$ frequency moments of dynamic structure factor, where s is the order of time derivatives of particle density taken in the extended basis set.[43] Extension of the initial basis sets by more slow dynamic variables in Eq. (12) up to the s'th integral of hydrodynamic variables additionally permits one to reproduce in the GCM representations $F_{ij}^{(N_v)}(k,t)$ the first $2s'+1$ time moments of corresponding time-correlation function.

For the case of transverse dynamics one can extend the initial basis set of transverse component of total mass current by slow dynamic variables in the same way. It is obvious that the transverse analogy for the regular density-density time-correlation functions can be achieved by introducing the functions constructed on slow extended dynamic variables

$$F_{ij}^T(k,t) = \langle I[J]_i^{T*}(k,0) I[J]_j^T(k,t)\rangle, \tag{16}$$

where the extended dynamic variable $I[J]_j^T(k,t)$ corresponds to the jth partial contribution to transverse strain. Obviously that the time Fourier transform of $F_{ij}^T(k,t)$ is the transverse analogy of dynamic structure factor [compare with Eq. (1)]. Therefore, using the extended GCM approach one can formally obtain the transverse analogy of the density-density time-correlation function $F_{ij}^T(k,t)$, its Fourier transform that is the transverse $S^T(k,\omega)$ and analyze leading mode contributions to their shape. Recently[24] it was shown that the transverse analogy of dynamic structure factor $S^T(k,\omega)$ calculated numerically from the relation in Eq. (1) contains pronounced

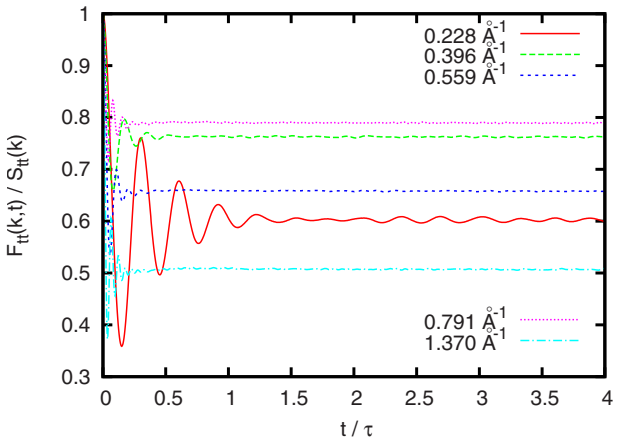

FIG. 1. (Color online) Normalized total density autocorrelation functions $F_{tt}(k,t)$ for $Mg_{70}Zn_{30}$ glass at room temperature. The time unit τ is equal to 1.688 ps.

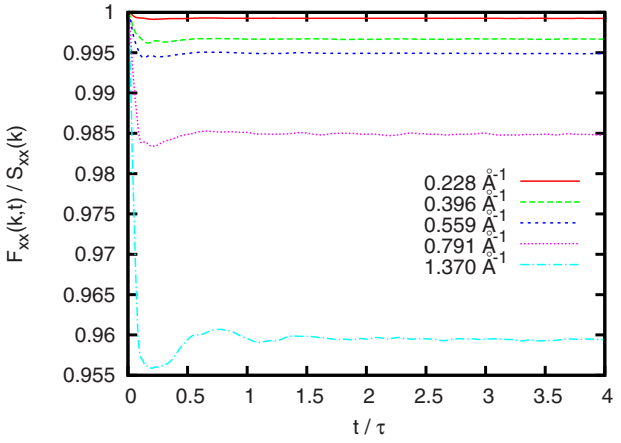

FIG. 2. (Color online) Normalized concentration density autocorrelation functions $F_{tt}(k,t)$ for $Mg_{70}Zn_{30}$ glass at room temperature. The time unit τ is equal to 1.688 ps.

peaks, which cannot be seen in the shape of transverse current spectral function $C^T(k,\omega)$.

One of the consequences of extending the basis set of dynamic variables by slow ones is more explicit description of non-Markovian effects. It was shown in Ref. 40 that the highest memory functions in the scheme with sets extended by slow variables are not anymore Markovian and take into account slow frequency-dependent processes. Hence, one can expect that the extended GCM scheme can be useful for treatment of collective dynamics in glass systems. To date the original scheme of systematic improvement of theoretical description of collective dynamics by taking into account both frequency moments of spectral functions and time moments of time-correlation functions, proposed in Ref. 40, was applied just to studies of polarization modes[40] and generalized shear viscosity[41] in water. However, this approach has never been applied to studies of acoustic excitations in liquids or glasses.

In summary, the reported here scheme for analysis of MD-derived time-correlation functions of the glass systems consists in several steps: (i) MD simulations permit to obtain time evolution of all hydrodynamic (conserved) variables and short-time (nonconserved) nonhydrodynamic ones; (ii) from calculated hydrodynamic time-correlation functions one estimates nonergodicity factors $f_{ij}(k)$; (iii) from the time-correlation functions shifted by $f_{ij}(k)$ one calculates all the matrix elements of $\mathbf{T}(k)$ on slow dynamic variables like Eq. (13); (iv) for each k-point sampled in MD simulations one solves the eigenvalue problem for the generalized hydrodynamic matrix $\mathbf{T}(k)$, estimates spectrum of eigenmodes and performs analysis of corresponding EGCM representations Eq. (15) for MD-derived time-correlation functions.

IV. RESULTS AND DISCUSSION

A. Time-correlation functions

The total density $F_{tt}(k,t)$ and mass-concentration density $F_{xx}(k,t)$ autocorrelation functions obtained in MD simulations of Mg_{70}-Zn_{30} glass are shown in Figs. 1 and 2, respectively. Both types of time-correlation functions have stable plateau on large times due to structural arrest of particles, that correspond to the nonergodicity factors $f_{ii}(k)$, $i=t,x$. The total density autocorrelation functions $F_{tt}(k,t)$ contain fast damped oscillations, the frequency of which increases with wave number k. These are the oscillations due to sound propagation. One cannot observe other oscillating processes with smaller than acoustic mode frequency, which would visibly affect the shape of $F_{tt}(k,t)$ time-correlation functions.

In contrast to the total density autocorrelation functions the time-correlation functions $F_{xx}(k,t)$ do not show visible contributions from sound excitations, however, they contain a shallow smeared minimum at the time ~0.4 ps. The damped oscillations in the shape of density-density time-correlation functions are usually an evidence of some damped collective propagating process. And what is remarkable, the frequency of the overdamped oscillations in the shape of $F_{xx}(k,t)$ is definitely smaller than for the case of sound excitations seen on the shape of $F_{tt}(k,t)$ and practically independent of k.

In order to estimate what kind of collective modes contribute to the time-correlation functions $F_{tt}(k,t)$ and $F_{xx}(k,t)$ let us analyze first the shape of corresponding total and concentration dynamic structure factors and later apply the proposed above EGCM scheme for their theoretical analysis.

B. Numerical analysis of dynamic structure factors

The total and concentration dynamic structure factors were obtained numerically as Fourier-transformed time-correlation functions with subtracted nonergodicity factors: $F_{tt}(k,t)-f_{tt}(k)$ and $F_{xx}(k,t)-f_{xx}(k)$, respectively. The transverse dynamic structure factors were obtained from the transverse total and concentration current spectral functions according to the relation in Eq. (1). The dynamic structure factors and their transverse counterparts are shown for several wave numbers in Fig. 3.

Density of vibrational states $D(\omega)$ obtained in a standard way via Fourier-transformed velocity autocorrelation func-

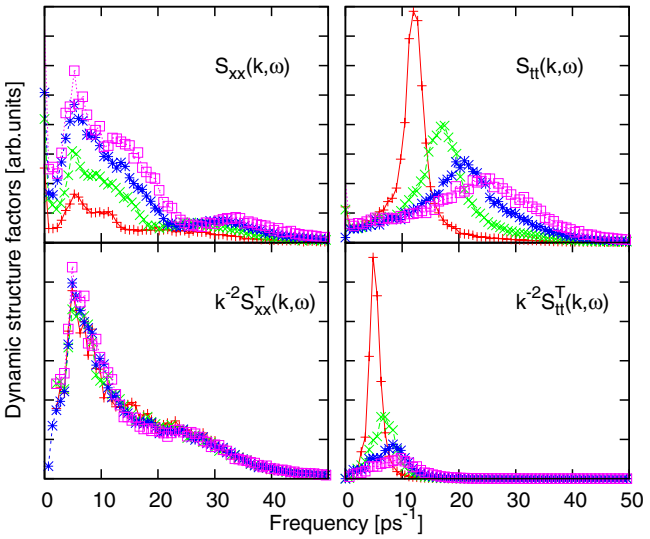

FIG. 3. (Color online) Total and concentration longitudinal and transverse dynamic structure factors for $Mg_{70}Zn_{30}$ glass at room temperature for several wave numbers: $k=0.23$ Å^{-1} (plus), $k=0.32$ Å^{-1} (cross), $k=0.40$ Å^{-1} (star), and $k=0.47$ Å^{-1} (box).

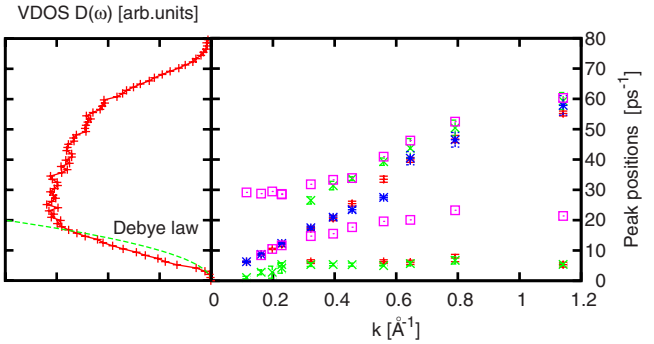

FIG. 4. (Color online) Density of vibrational states in $Mg_{70}Zn_{30}$ glass at room temperature and an excess over the Debye law (dashed line in the left frame) with dispersion curves of longitudinal excitations, obtained from peak positions of dynamic structure factors $S_{tt}(k,\omega)$ (plus symbols), $S_{xx}(k,\omega)$ (cross symbols) and corresponding current spectral functions $C^{L}_{tt}(k,\omega)$ (stars) and $C^{L}_{xx}(k,\omega)$ (boxes).

tions is shown in the left frame of Fig. 4. The calculated$D(\omega)$ gives evidence that in the frequency range $\sim 3-15$ ps^{-1} there exists an excess of vibrational states over the Debye law. This feature of the vibrational density of states is in complete agreement with experimental data[44] on $Mg_{70}Zn_{30}$ glass at room temperature from the time-of-flight measurements. In the right frame of Fig. 4 we show the dispersion of longitudinal collective modes obtained as peak positions of the dynamic structure factors $S_{ii}(k,\omega)$, $i=t,x$, that permits visual comparison of frequency ranges of different collective modes and their contributions to the density of vibrational states. The excess in density of states is caused by some low-frequency collective modes, which are clearly seen as corresponding peaks at the concentration dynamic structure factors $S^{L,T}_{xx}(k,\omega)$ shown in Fig. 3. All the low-frequency peaks of $S^{L,T}_{xx}(k,\omega)$ have asymmetric shape that is known as one of the features of boson-peak modes.

The total dynamic structure factors due to strong contribution from the sound excitations cannot be used for estimation of the dispersion of the low-frequency excitations. Since the concentration dynamic structure factors do not reflect in the long-wavelength region the processes connected with total density fluctuations it appears, that one of the most extremely important consequences of $S^{L,T}_{xx}(k,\omega)$ is a possibility to trace down to the smallest wave numbers the dispersion of the modes that are responsible for boson peak. Moreover this even implies that the boson peak is not caused by acoustic excitations but some collective processes specific for glasses. In particular, it is seen in Fig. 4 that the low-frequency modes were observed on the shape of $S^{L,T}_{xx}(k,\omega)$ down to the smallest wave numbers, although there is a clear tendency of almost linear reduction in their frequency in the long-wavelength region that implies absence of these collective modes on macroscopic distances. Existence of the boson-peak modes at smallest wave numbers means, that they cannot correspond to strongly localized vibrational states and their spatial extent is of order 20 Å.

Concentration dynamic structure factors $S^{L,T}_{xx}(k,\omega)$ contain also smeared out high-frequency maxima (shoulders in transverse case) located approximately at the frequency ~ 30 ps^{-1} that correspond to opticlike excitations in the binary glass. This is a specific feature of dynamic structure factors for binary glass systems because in liquids the concentration dynamic structure factors in hydrodynamic regime do not contain any side peaks and reflect solely contribution from relaxation processes connected with mutual diffusion. One may assume that this specific behavior is caused by coupling of opticlike modes with ultraslow boson-peak modes.

C. GCM representations of time-correlation functions

The EGCM representations of time-correlation functions are represented in analytical form via Eq. (15). The EGCM analysis of MD-derived time-correlation functions makes sense only in the case when the corresponding EGCM functions describe the MD data with good precision. The quality of EGCM representations is provided by several frequency and time moments, identical for MD-derived time-correlation functions and theoretical expression (15).

For the case of binary systems studied by the extended GCM approach one has to reproduce frequency and time moments of corresponding partial dynamic structure factors and partial density-density time-correlation functions. We have found that the two levels of hierarchy of slow processes, i.e., the highest level of the ultraslow dynamic variables in Eq. (12) was restricted by the second time integral of hydrodynamic variables, taken in the extended basis set were sufficient for accurate description of partial density-density time-correlation functions in glasses. In Fig. 5 we show the quality of EGCM representations (dashed lines) for partial density autocorrelation functions (solid lines) obtained within the ten-variable extended dynamic model

$$\mathbf{A}^{(10)}(k,t) = \{I^2[n]_A(k,t), I^2[n]_B(k,t), I[n]_A(k,t), I[n]_B(k,t), n_A(k,t), n_B(k,t), J_A^L(k,t), J_B^L(k,t), \dot{J}_A^L(k,t), \dot{J}_B^L(k,t)\}. \quad (17)$$

For comparison the GCM representations obtained in Markovian approximation within the standard VE six-variable model Eq. (10) (Refs. 45 and 46) are shown by dotted lines. Such VE dynamic model usually enabled one to reproduce correctly the partial density-density time-correlation functions in binary liquids. However, as it is seen from Fig. 5 in the case of glasses the standard viscoelastic model in Markovian approximation essentially underestimates damping of collective excitations, and this is responsible for strong oscillations of GCM representations shown in Fig. 5 by dotted lines while the short-time description of $F'_{ij}(k,t)$ provided by first five frequency moments of partial dynamic structure factors is very good. Only inclusion of slow dynamic variables in Eq. (12) into the general scheme and taking into account non-Markovian effects induced in the memory functions by treatment of these dynamic variables permits to reproduce nicely the partial density-density time-correlation functions in $Mg_{70}Zn_{30}$ glass. The different periods of damped oscillations observed in the shape of both partial density autocorrelation functions give evidence on existence of at least two types of collective excitations in the binary glass. This will be discussed in more details below when the spectra of collective excitations are analyzed. We would like to make a reminder that there is no fit with any adjustable parameters in this GCM analysis—just the analysis of results for different dynamic models, that provide an information on the dynamic eigenmodes existing in the system.

Transverse dynamics in glasses is even more difficult for treatment within the GCM approach than the longitudinal case. Large (almost infinite) shear viscosity is responsible for extremely small transverse correlation times, that yields almost nondamped oscillations for theoretical representations of partial transverse current-current time-correlation functions when the GCM treatment is performed within the standard four-variable viscoelastic model of transverse dynamics.[34] In Fig. 6 the viscoelastic representations are shown by dotted line and this is again an evidence of inapplicability of the regular GCM approach to glass dynamics. In order to keep the same level of treatment of ultraslow processes as in the longitudinal case we extend the initial viscoelastic basis set of transverse dynamic variables by the following three levels of hierarchy of slow dynamic variables with respect to partial transverse currents:

$$\mathbf{A}^{(10T)}(k,t) = \{I^3[J]_A^T(k,t), I^3[J]_B^T(k,t), I^2[J]_A^T(k,t), I^2[J]_B^T(k,t), I[J]_A^T(k,t), I[J]_B^T(k,t), J_A^T(k,t), J_B^T(k,t), \dot{J}_A^T(k,t), \dot{J}_B^T(k,t)\}. \quad (18)$$

We would like to make a reminder, that according to Eq. (16) the first level of ultraslow dynamic variables yields transverse analogy of particle density. Therefore the extended basis set $\mathbf{A}^{(10T)}(k,t)$ corresponds, in fact, to the same level of approximation as it was chosen for the longitudinal case.

The theoretical representations for the transverse partial current-current correlation functions are shown in Fig. 6 by dashed lines. In general the agreement between MD-derived time-correlation functions and theoretical GCM representations, obtained within the dynamic model $\mathbf{A}^{(10T)}(k,t)$ is very good. The theoretical curves correctly reproduce the oscillations as well as their damping for all three partial transverse functions.

D. Spectra of propagating longitudinal and transverse eigenmodes

Complex-conjugated pairs of eigenvalues

$$z_\alpha^{\pm}(k) = \sigma_\alpha(k) \pm i\omega_\alpha(k)$$

correspond in the GCM approach to the collective excitations, that can propagate in the system with dispersion $\omega_\alpha(k)$ and damping $\sigma_\alpha(k)$, and this permits to study specific features of dispersion and damping of collective modes in various systems.

In Fig. 7 the dispersion of different propagating longitudinal eigenmodes in binary metallic $Mg_{70}Zn_{30}$ glass is shown. Two high-frequency branches of collective excitations can be immediately identified in the region $k < 0.4$ Å^{-1} as dispersion of acoustic (crosses) and opticlike (pluses) excitations. In contrast to liquids the opticlike modes in glasses are well-defined collective excitations, as it was shown on example of $Mg_{70}Zn_{30}$ glass in Ref. 15. In general, our results for the high-frequency modes is in agreement also with other simulations studies of disordered solids.[17,18]

The imaginary parts of longitudinal eigenvalues correspond well to the peaks positions of the total and concentration spectral functions shown in Fig. 4. For wave numbers $k > 0.4$ Å^{-1} the two branches show a crossover to the region where the corresponding high- and low-frequency branches reflect dynamics of mainly light (Mg) and heavy (Zn) species of the binary glass, respectively.

Among the complex-conjugated pairs of eigenvalues obtained for $Mg_{70}Zn_{30}$ glass within the ten-variable dynamic model Eq. (17) there appeared eigenmodes with very low frequencies, shown in Fig. 7 by stars and boxes. Interesting,

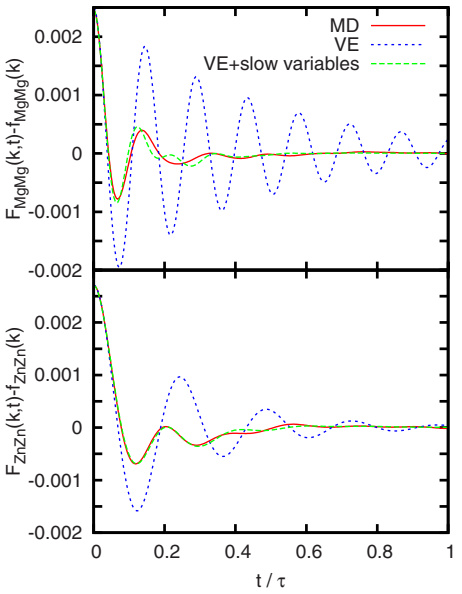

FIG. 5. (Color online) Partial density autocorrelation functions for $Mg_{70}Zn_{30}$ glass for $k=0.396$ Å^{-1} at room temperature: MD-derived functions—solid lines, EGCM representations obtained within regular VE approximation $\mathbf{A}^{(6)}$—dotted lines, and EGCM representations from extended by slow dynamic variables viscoelastic model Eq. (17)—dashed lines. The time scale τ is equal to 1.688 ps.

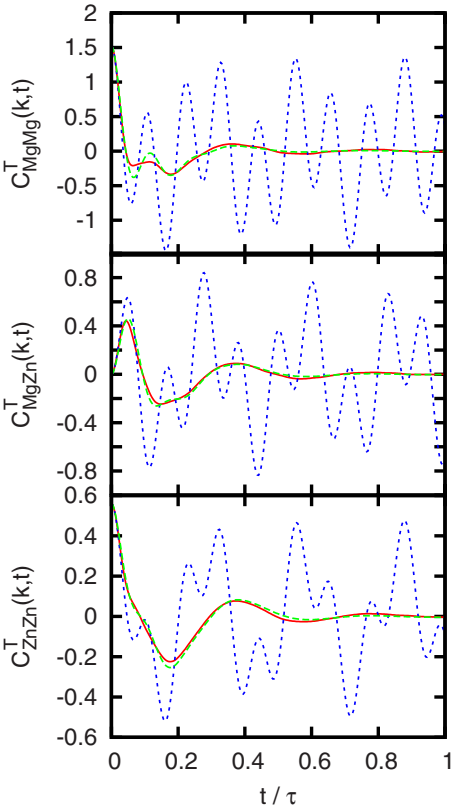

FIG. 6. (Color online) Comparison of theoretical representations with MD-derived partial transverse current-current time-correlation functions for $Mg_{70}Zn_{30}$ glass at $k=0.396$ Å^{-1} at room temperature: MD-derived functions—solid lines, GCM representations obtained within four-variable VE approximation $\mathbf{A}^{(4T)}$—dotted lines, and GCM representations from the extended by slow dynamic variables viscoelastic model Eq. (18)—dashed lines. The time scale τ is equal to 1.688 ps.

that for $Mg_{70}Zn_{30}$ glass the low-frequency excess of vibrational states over the Debye law known as boson peak is observed in the region $\sim 4-5$ ps^{-1}, that coincides with the frequencies of obtained ultraslow dynamic eigenmodes. It seems that these two ultralow-frequency branches are connected mainly with total density and concentration fluctuations, respectively, however, this should be studied in future in more details. It can be judged from the tendency of dispersion of the ultralow-frequency eigenmodes, that in the long-wavelength limit they will be absent in the spectrum. In its turn this means a restricted spatial region of existence of these modes, i.e., quite localized origin of the ultralow-frequency dynamic eigenmodes.

The real parts of complex eigenvalues $\sigma_\alpha(k)$ correspond to damping of collective excitations. In Fig. 8 we show the wave-number dependence of damping in the long-wavelength region for three main branches of propagating excitations shown by the same symbols as their dispersion in Fig. 7. The issue of long-wavelength asymptote of acoustic excitations in glasses is very controversial in the literature. There are evidences of k^2 and k^4 regions for damping of long-wavelength acoustic excitations. Our fit-free EGCM results shown by symbols in Fig. 8 permit to conclude that sound damping in the long-wavelength region is a quadratic function of wave number with damping coefficient $\Gamma = 26$ Å^2/ps. However, there is another branch of ultraslow boson-peak modes with comparable values of damping in the long-wavelength region. As it is seen from Fig. 8 the damping of boson-peak modes increases much faster than a k^2 dependence drawn through the lowest k point. The third $\sigma_\alpha(k)$ dependence shown in Fig. 8 corresponds to the high-frequency opticlike modes and tends to a nonzero constant in the long-wavelength limit. Another conclusion can be made from comparison of dispersion and damping of acoustic excitations in the long-wavelength region: for the $Mg_{70}Zn_{30}$ glass the Ioffe-Regel criterion $\omega_{sound}/\pi = \sigma$ will be satisfied at the frequencies that several times exceed the frequency of the boson peak. This declines the possibility for overdamped longitudinal acoustic modes to form boson peak in $Mg_{70}Zn_{30}$ glass. Our finding is in agreement with similar results reported for the $NiZr_2$ metallic glass.[47]

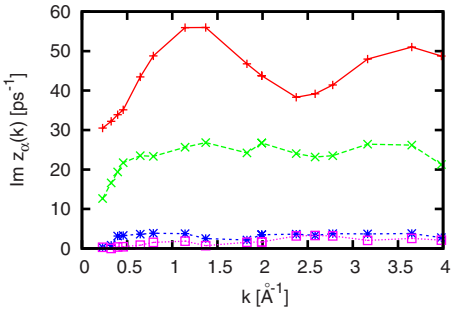

FIG. 7. (Color online) Dispersion of generalized propagating longitudinal eigenmodes for the $Mg_{70}Zn_{30}$ glass at room temperature as obtained within the extended dynamic model $\mathbf{A}^{(10)}(k,t)$.

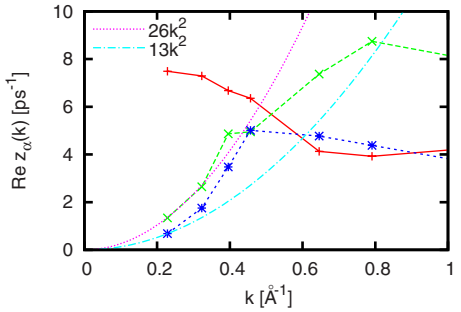

FIG. 8. (Color online) Damping of generalized propagating longitudinal eigenmodes in the long-wavelength region for the $Mg_{70}Zn_{30}$ glass at room temperature as obtained within the extended dynamic model $\mathbf{A}^{(10)}(k,t)$.

For the case of transverse dynamics we have obtained within the ten-variable extended dynamic modes $\mathbf{A}^{(10T)}(k,t)$ four pairs of complex-conjugated pairs of eigenvalues too. The dispersion of corresponding transverse collective propagating modes is shown in Fig. 9. One can definitely say that in the region $k<0.7$ Å^{-1} the low- and high-frequency branches shown by plus and cross symbol-connected lines correspond to transverse acoustic and optic modes, respectively, while in the region $k>1.2$ Å^{-1} these branches reflect transverse dynamics of mainly heavy (Zn) and light (Mg) components of the binary glass, respectively. Again, as for the case of longitudinal dynamics we obtained two pairs of transverse complex-conjugated eigenvalues with very low frequencies, that were a little smaller than the corresponding longitudinal ones. The same tendency as in the longitudinal case is observed for the transverse ultraslow modes: in the long-wavelength region their frequency drops with decreasing wave number.

Damping of transverse modes, represented as real parts of complex eigenvalues, are shown in Fig. 10. Transverse acoustic excitations show almost quadratic in wave-number behavior in long-wavelength region and by comparison with longitudinal acoustic modes shown in Fig. 8 their damping coefficient is a bit smaller, $\Gamma^T=22$ Å^2/ps. The transverse ultraslow modes have comparable damping to the acoustic modes. In general, the damping of transverse ultraslow modes is smaller that in the case of longitudinal Boson-peak modes. The damping of transverse opticlike excitations in contrast to longitudinal optic modes decreases toward the

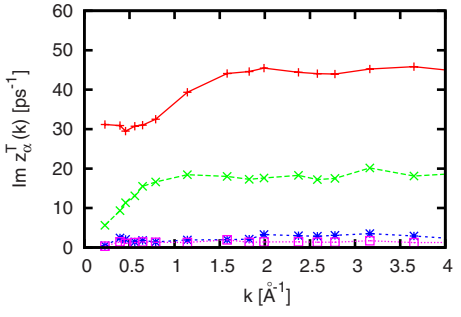

FIG. 9. (Color online) Dispersion of generalized propagating transverse eigenmodes for the $Mg_{70}Zn_{30}$ glass at room temperature as obtained within the extended dynamic model $\mathbf{A}^{(10T)}(k,t)$.

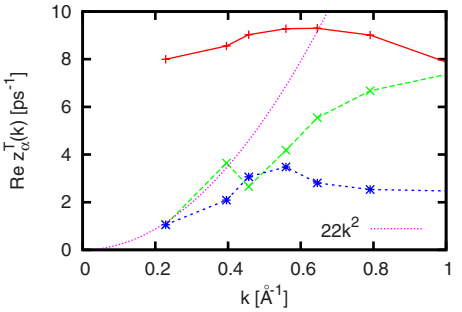

FIG. 10. (Color online) Damping of generalized propagating transverse eigenmodes for the $Mg_{70}Zn_{30}$ glass at room temperature as obtained within the extended dynamic model $\mathbf{A}^{(10T)}(k,t)$.

long wavelengths, however, tends to the same value ~ 7.5 ps^{-1} in $k\to 0$ limit. We also stress that dispersion of the long-wavelength longitudinal and transverse optic modes tends to the same frequency $\omega_{opt}^{L,T}(0)\sim 30$ ps^{-1} as it must be for systems without long-range interaction.

E. Mode contributions to dynamic structure factors and transverse current spectral functions

The eigenvectors associated with corresponding collective mode $z_\alpha(k)$ yield very important information on wave-number-dependent contributions of different collective modes to various dynamic structure factors. Since the density-density time-correlation functions and dynamic structure factors are related by the time Fourier transform the same amplitudes of wave-number-dependent contributions from different dynamic eigenmodes correspond to the damping oscillatory behavior of a time-correlation function and the side peaks of relevant dynamic structure factor. The EGCM expression for representation of density-density time-correlation function Eq. (15) contains complex weight coefficients $G_{ij}^{\alpha}(k)$, that are calculated straightforward from the eigenvectors associated with the αth dynamic eigenmode. An equivalent expression for the normalized EGCM representations with real weight coefficients within the applied ten-variable dynamic model reads as follows:

$$\frac{F_{ij}^{(10)'}(k,t)}{F_{ij}'(k)} = \sum_{\alpha=1}^{2} A_{ij}^{\alpha}(k)e^{-d_\alpha(k)t} + \sum_{\alpha=1}^{4}\{B_{ij}^{\alpha}(k)\cos[\omega_\alpha(k)t] + D_{ij}^{\alpha}(k)\sin[\omega_\alpha(k)t]\}e^{-\sigma_\alpha(k)t}, \quad (19)$$

where $A_{ij}^{\alpha}(k)$ are the amplitudes of contributions from the nonpropagating relaxing modes while $B_{ij}^{\alpha}(k)$ and $D_{ij}^{\alpha}(k)$ are the amplitudes of symmetric and asymmetric contributions from the αth propagating mode, respectively. The real coefficients $B_{ij}^{\alpha}(k)$ and $D_{ij}^{\alpha}(k)$ appear as linear combinations of corresponding complex weight coefficients $G_{ij}^{\alpha}(k)$ in a similar way as it is in hydrodynamic theory[48] because expression (19) is a straightforward extension of hydrodynamic time-correlation functions that follows from the GCM approach (see Ref. 49 for details). Namely, the amplitudes $B_{ij}^{\alpha}(k)$ and $D_{ij}^{\alpha}(k)$ correspond to the strength of Lorentzian and non-Lorentzian contributions to the αth side peak of dynamic structure factors

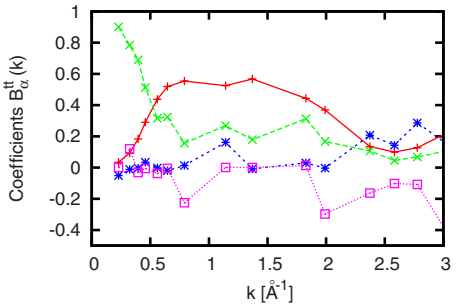

FIG. 11. (Color online) Coefficients of symmetric $B^{\alpha}_{tt}(k)$ contributions of generalized propagating eigenmodes to the total density autocorrelation functions as obtained from corresponding eigenvectors within the extended dynamic model $\mathbf{A}^{(10)}(k,t)$.

$$\frac{S_{ij}(k,\omega)}{S_{ij}(k)-f_{ij}(k)} = \sum_{\alpha=1}^{2} A^{\alpha}_{ij}(k)\frac{2d_{\alpha}(k)}{\omega^2+d^2_{\alpha}(k)} + \sum_{\pm,\alpha=1}^{4}\left[B^{\alpha}_{ij}(k)\frac{\sigma_{\alpha}(k)}{[\omega\pm\omega_{\alpha}(k)]^2+\sigma^2_{\alpha}(k)} \pm D^{\alpha}_{ij}(k)\frac{\omega\pm\omega_{\alpha}(k)}{[\omega\pm\omega_{\alpha}(k)]^2+\sigma^2_{\alpha}(k)}\right]. \quad (20)$$

It is seen from Eq. (20) that the non-Lorentzian contribution with the amplitude $D^{\alpha}_{ij}(k)$ changes its sign right at the frequency $\omega=\omega_{\alpha}$ thus causing the asymmetry of the αth side peak of dynamic structure factor $S_{ij}(k,\omega)$. Since in Fig. 3 the MD-derived concentration dynamic structure factors clearly reveal asymmetric form of the contributions coming from the boson-peak modes one can expect to see this effect in the strength of non-Lorentzian (asymmetric) contributions based on the EGCM analysis.

In Figs. 11 and 12 we show the wave-number-dependent contributions from four branches of collective excitations shown with the same symbols as their dispersion curves in Fig. 7. Contributions $B^{\alpha}_{tt}(k)$ from the propagating modes to the total density autocorrelation functions and $S_{tt}(k,\omega)$ in the long-wavelength region are solely coming from acoustic excitations. The contribution of opticlike modes increases from long-wavelength region almost as k^2 up to the wave number ~ 0.5 Å^{-1}, where according to dispersion curves in Fig. 7 a cross section of acoustic and optic branches is possible. However, it is not an easy task to separate contributions for $k>0.5$ Å^{-1} and assign them solely to acoustic or optic modes because in that region of wave numbers the high- and low-frequency branches reflect mainly the dynamics of light (Mg) and heavy (Zn) components of the binary glass. It is seen that the ultralow-frequency modes, that are located in the frequency range of boson peak, contribute marginally to the shape of total dynamic structure factors, that is in agreement with MD data shown in Fig. 3. The asymmetric contributions $D^{\alpha}_{tt}(k)$ in the region $k<2$ Å^{-1} are very small for all the propagating eigenmodes giving evidence of almost Lorentzian shapes of leading contributions to $S_{tt}(k,\omega)$, that is in agreement with MD-derived $S_{tt}(k,\omega)$ shown in Fig. 3.

For the case of concentration density autocorrelation functions (and concentration dynamic structure factors) the

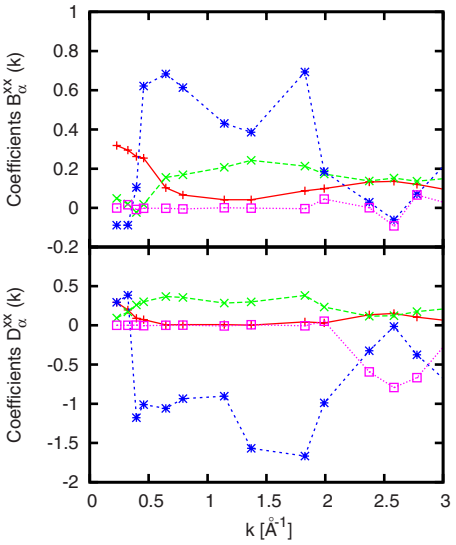

FIG. 12. (Color online) Coefficients of symmetric $B^{\alpha}_{xx}(k)$ and asymmetric $D^{\alpha}_{xx}(k)$ contributions of generalized propagating eigenmodes to the concentration density autocorrelation functions as obtained from corresponding eigenvectors within the extended dynamic model $\mathbf{A}^{(10)}(k,t)$. The line-connected symbols correspond to the same excitations as in Fig. 11.

wave-number dependence of mode contributions is completely different. Now, the leading contribution to the shape of $F_{xx}(k,t)$ comes from the ultralow-frequency modes associated with the boson peak while in the long-wavelength region acoustic excitations do not contribute at all to the $F_{xx}(k,t)$ and some contribution comes from the opticlike excitations. It is remarkable that the analysis of mode contributions, obtained from the fit-free EGCM analysis, permits to associate the slow overdamped oscillations in the shape of $F_{xx}(k,t)$ as it was shown in Fig. 2 to the boson-peak modes. This completely supports our finding from the solely numerical analysis of MD data that the low-frequency peak positions of the $S_{xx}(k,\omega)$ can be used for estimation of dispersion of the boson peak modes shown in Fig. 4. Remarkable that in contrast to the EGCM results on asymmetric contributions to the total dynamic structure factors $S_{tt}(k,\omega)$ the coefficients $D^{\alpha}_{xx}(k)$ from the boson-peak modes are large, that means essentially asymmetric shape of peaks of $S_{xx}(k,\omega)$, that was really observed in MD simulations (see Fig. 3).

For the case of transverse dynamics the main contributions to the shape of transverse current spectral functions come form transverse acoustic and optic modes, that is shown in Figs. 13 and 14. It is seen that in the region $k<0.7$ Å^{-1} the total and concentration spectral functions represent solely contributions from transverse acoustic and optic modes, respectively. For larger wave numbers both branches contribute to the shape of $C^{T}_{tt}(k,\omega)$ and $C^{T}_{xx}(k,\omega)$. Both branches of transverse ultraslow modes do not show a visible effect on the shape of transverse current spectral functions. However, they contribute to the transverse analogies of the dynamic structure factors, as it is shown in Fig. 3. Analytical study of contributions to the $S^{T}_{tt}(k,\omega)$ and $S^{T}_{xx}(k,\omega)$ will be made elsewhere.

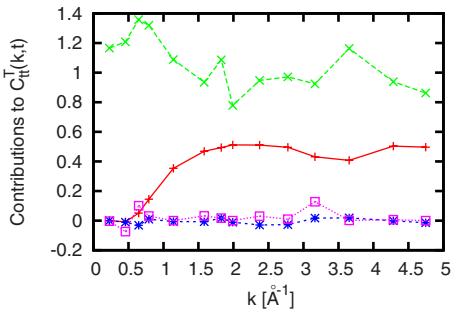

FIG. 13. (Color online) Contributions of generalized propagating transverse eigenmodes to the total transverse current autocorrelation functions as obtained from corresponding eigenvectors within the extended dynamic model $\mathbf{A}^{(10T)}(k,t)$. The line-connected symbols correspond to the same excitations as in Fig. 9.

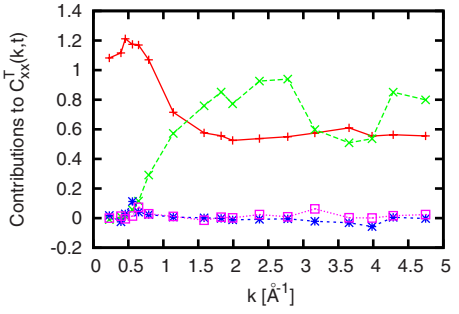

FIG. 14. (Color online) Contributions of generalized propagating transverse eigenmodes to the concentration transverse current autocorrelation functions as obtained from corresponding eigenvectors within the extended dynamic model $\mathbf{A}^{(10T)}(k,t)$. The line-connected symbols correspond to the same excitations as in Fig. 9.

V. CONCLUSIONS

We have shown how the extended GCM approach can be applied for a fit-free analysis of collective dynamics in glasses. The idea of making use of time moments of time-correlation functions[40] appeared to be very fruitful, namely, for extension of the GCM methodology on glass systems for two reasons: (i) slow dynamic variables different from the regular hydrodynamic ones are included into the GCM scheme and (ii) non-Markovian effects are taken into account. Our first attempt of analysis of collective excitations within the extended GCM approach is demonstrated on the case of a binary metallic $Mg_{70}Zn_{30}$ glass. Main conclusions of this study can be formulated as follows.

(i) We have found pronounced low-frequency peaks in MD-derived concentration dynamic structure factors as well as in their transverse analogues. This permitted us to trace down to small wave numbers the dispersion of low-frequency modes that was impossible by analysis of only total dynamic structure factors. It is shown that the low-frequency modes are located right at the frequencies of the excess of vibrational density of states (boson peak).

(ii) Strong manifestation of the low-frequency modes, namely, in the shape of concentration dynamic structure factors implies their nonacoustic origin because usually the acoustic modes contribute strongly to total dynamic structure factors, while opticlike modes—to the concentration spectral functions.

(iii) We have proposed an extended GCM approach (EGCM), that permits estimation of the dynamic eigenmodes and associated eigenvectors in glass systems.

(iv) Two levels of hierarchy of slow dynamic variables, $I[n]_i(k,t)$ and $I^2[n]_i(k,t)$, is enough to reproduce with good quality MD-derived partial density-density time-correlation functions in the studied two-component glass systems. For the case of transverse dynamics perfect reproduction of the partial transverse time-correlation functions was achieved within extension to three levels of hierarchy of slow dynamic variables [down to $I^3[J]^T_i(k,t)$] that corresponded, in fact, to the same level of approximation as in the longitudinal case.

(v) Extended slow dynamic variables lead to emergence of low-frequency complex eigenmodes with very flat dispersion, which can be responsible for formation of a low-frequency excess on vibrational density of states over the Debye law known as boson peak.

(vi) The damping of acoustic eigenmodes was obtained to follow quadratic dependence $\sim k^2$ in the long-wavelength limit while damping of the boson-peak modes showed much faster increase with wave numbers.

(vii) Analysis of mode contributions to dynamic structure factors performed by the EGCM approach gives evidence of strong contributions of boson-peak modes to the concentration dynamic structure factors, that is in agreement with MD data. The EGCM approach correctly reflects the strong asymmetric part of contributions from the boson-peak modes to $S_{xx}(k,\omega)$.

The extended GCM approach opens broad perspectives in exploration of collective excitations in glasses. In particular the hot issues to be focused on in the future EGCM studies of glass systems are: the origin of boson peak modes, main features of dispersion and damping of longitudinal and transverse collective excitations in glasses, wave-number dependence of contributions from different collective modes to experimentally measured intensities of scattered x-rays or neutrons. In order to estimate the origin of boson-peak modes one can apply within the EGCM approach a projection technique for dynamic variables onto different kinds of collective processes. Such a projection technique was successfully applied in the case of liquids for estimation of origin of nonhydrodynamic collective modes in liquids such as opticlike modes,[34] heat waves,[33] and structural relaxation.[50]

ACKNOWLEDGMENTS

T.B. was supported by the Joint SFBRU-RFBR Program under Project No. Φ28.2/037. The allocation time at the SCIT3 supercomputer at Institute of Cybernetics of NASU is acknowledged.

[1] W. Götze, in *Liquids, Freezing and the Glass Transition*, edited by J.-P. Hansen, D. Levesque, and J. Zinn-Justin (Elsevier, Amsterdam, 1991).
[2] W. Götze, *Complex Dynamics of Glass-Forming Liquids - A Mode-Coupling Theory* (Oxford University Press, Oxford, 2009).
[3] W. Kob and H. C. Andersen, Phys. Rev. E **51**, 4626 (1995); **52**, 4134 (1995).
[4] W. Götze and M. R. Mayr, Phys. Rev. E **61**, 587 (2000).
[5] W. Schirmacher, E. Maurer, and M. Pöhlmann, Phys. Status Solidi C **1**, 17 (2004).
[6] W. Schirmacher, G. Ruocco, and T. Scopigno, Phys. Rev. Lett. **98**, 025501 (2007).
[7] U. Buchenau and H. R. Schober, Philos. Mag. **88**, 3885 (2008).
[8] W. Schirmacher, C. Tomaras, B. Schmid, G. Baldi, G. Viliani, G. Ruocco, and T. Scopigno, Condens. Matter Phys. **13**, 23606 (2010).
[9] S. N. Taraskin and S. R. Elliott, J. Phys.: Condens. Matter **11**, A219 (1999).
[10] T. S. Grigera, V. Martin-Mayor, G. Parisi, and P. Verrocchio, Nature (London) **422**, 289 (2003).
[11] U. Buchenau, Yu. M. Galperin, V. L. Gurevich, D. A. Parshin, M. A. Ramos, and H. R. Schober, Phys. Rev. B **46**, 2798 (1992).
[12] S. N. Taraskin and S. R. Elliott, Europhys. Lett. **39**, 37 (1997).
[13] V. Lubchenko and P. G. Wolynes, Proc. Natl. Acad. Sci. U.S.A. **100**, 1515 (2003).
[14] C. Cohen, P. D. Fleming, and J. H. Gibbs, Phys. Rev. B **13**, 866 (1976).
[15] J. Hafner, J. Phys. C **16**, 5773 (1983).
[16] J. Horbach, W. Kob, and K. Binder, Eur. Phys. J. B **19**, 531 (2001).
[17] E. Enciso, N. G. Almarza, M. A. Gonzalez, F. J. Bermejo, R. Fernandez-Perea, and F. Bresme, Phys. Rev. Lett. **81**, 4432 (1998).
[18] R. Fernandez-Perea, F. J. Bermejo, J. L. Martinez, E. Enciso, and P. Verkerk, Phys. Rev. E **59**, 3212 (1999).
[19] N. Anento and J. A. Padró, Phys. Rev. B **70**, 224211 (2004).
[20] B. B. Laird and H. R. Schober, Phys. Rev. Lett. **66**, 636 (1991).
[21] S. N. Taraskin and S. R. Elliott, Phys. Rev. B **56**, 8605 (1997).
[22] G. Ruocco, F. Sette, R. Di Leonardo, G. Monaco, M. Sampoli, T. Scopigno, and G. Viliani, Phys. Rev. Lett. **84**, 5788 (2000).
[23] T. Scopigno, G. Ruocco, and F. Sette, Rev. Mod. Phys. **77**, 881 (2005).
[24] H. Shintani and H. Tanaka, Nature Mater. **7**, 870 (2008).
[25] G. Monaco and S. Mossa, Proc. Natl. Acad. Sci. U.S.A. **106**, 16907 (2009).
[26] J.-P. Boon and S. Yip, *Molecular Hydrodynamics* (McGraw-Hill, New York, 1980).
[27] U. Balucani and M. Zoppi, *Dynamics of the Liquid State* (Clarendon Press, Oxford, 1994).
[28] I. M. deSchepper, E. G. D. Cohen, C. Bruin, J. C. van Rijs, W. Montfrooij, and L. A. de Graaf, Phys. Rev. A **38**, 271 (1988).
[29] I. M. Mryglod, Condens. Matter Phys. **1**, 753 (1998).
[30] T. Bryk and I. Mryglod, Condens. Matter Phys. **11**, 139 (2008).
[31] T. Bryk and J.-F. Wax, J. Chem. Phys. **132**, 074504 (2010).
[32] T. Bryk and I. Mryglod, J. Phys.: Condens. Matter **12**, 3543 (2000).
[33] T. Bryk and I. Mryglod, Phys. Rev. E **63**, 051202 (2001).
[34] T. Bryk and I. Mryglod, J. Phys.: Condens. Matter **12**, 6063 (2000).
[35] T. Bryk and I. Mryglod, J. Phys.: Condens. Matter **14**, L445 (2002).
[36] J. Bosse, G. Jacucci, M. Ronchetti, and W. Schirmacher, Phys. Rev. Lett. **57**, 3277 (1986).
[37] T. Bryk and I. Mryglod, J. Phys.: Condens. Matter **17**, 413 (2005).
[38] T. Bryk and J.-F. Wax, Phys. Rev. B **80**, 184206 (2009).
[39] P. H. K. de Jong, P. Verkerk, C. F. de Vroege, L. A. de Graaf, W. S. Howells, and S. M. Bennington, J. Phys.: Condens. Matter **6**, L681 (1994).
[40] I. P. Omelyan and M. V. Tokarchuk, J. Phys.: Condens. Matter **12**, L505 (2000).
[41] I. P. Omelyan, I. M. Mryglod, and M. V. Tokarchuk, Condens. Matter Phys. **8**, 25 (2005).
[42] A. B. Bhatia, D. E. Thornton, and N. H. March, Phys. Chem. Liq. **4**, 97 (1974).
[43] I. M. Mryglod, I. P. Omelyan, and M. V. Tokarchuk, Mol. Phys. **84**, 235 (1995).
[44] J.-B. Suck, H. Rudin, H.-J. Güntherodt, and H. Beck, J. Phys. C **14**, 2305 (1981).
[45] Ya. Chushak, T. Bryk, A. Baumketner, G. Kahl, and J. Hafner, Phys. Chem. Liq. **32**, 87 (1996).
[46] N. Anento, L. E. Gonzalez, D. J. Gonzalez, Ya. Chushak, and A. Baumketner, Phys. Rev. E **70**, 041201 (2004).
[47] T. Scopigno, J.-B. Suck, R. Angelini, F. Albergamo, and G. Ruocco, Phys. Rev. Lett. **96**, 135501 (2006).
[48] C. Cohen, J. W. H. Sutherland, and J. M. Deutch, Phys. Chem. Liq. **2**, 213 (1971).
[49] T. Bryk and I. Mryglod, J. Phys.: Condens. Matter **13**, 1343 (2001).
[50] T. Bryk and I. Mryglod, Phys. Rev. E **64**, 032202 (2001).